

# Buckling and d-Wave Pairing in HiTc-Superconductors

O. Jepsen, O.K. Andersen, I. Dasgupta, and S. Savrasov  
 Max-Planck Institut für Festkörperforschung, D-70569 Stuttgart, Germany

We have investigated whether the electron-phonon interaction can support a d-wave gap-anisotropy. On the basis of models derived from LDA calculations, as well as LDA linear-response calculations we argue that this is the case, for materials with buckled or dimpled CuO<sub>2</sub> planes, for the so-called buckling modes, which involve out-of-plane movements of the plane oxygens.

The mechanism of high-temperature superconductivity in hole-doped materials containing CuO<sub>2</sub> planes remains a subject of vivid debate.<sup>1</sup> A large amount of experimental data such as superconductivity-induced phonon renormalizations<sup>2</sup>, a large isotope effect away from optimal doping<sup>3</sup>, and phonon-related features in the tunnelling spectra<sup>4</sup> show effects of the electron-phonon interaction. Density-functional (LDA) calculations are in agreement with much of this, but indicate that the electron-phonon interaction has insufficient strength ( $\lambda_s \sim 1$ )<sup>5-8</sup> and leads to *s*-wave pairing. The experimental evidence that the symmetry of the paired state is *d*,<sup>9</sup> with lobes in the direction of the Cu-O bond, points to the Coulomb repulsion between two holes on the same copper site as the pairing agent. However, the scarcity of high-temperature superconducting materials, as well as results of Hubbard- and *t*-*J*-model calculations<sup>10</sup>, lead to the suspicion that something more than the Coulomb repulsion is needed.

It is therefore of interest<sup>11,12</sup> to investigate whether the electron-phonon interaction, which gives a negative (attractive) pair-interaction,  $V_{ep}(\mathbf{k}, \mathbf{k}') \propto -|g(\mathbf{k}, \mathbf{k}')|^2$ , could support the observed singlet- and *d*-wave pairing with the gap-anisotropy:  $\Delta(\mathbf{k}) \propto \cos(ak_x) - \cos(ak_y)$  sketched in Fig. 1. For this to occur, and assuming a BCS-like zero-temperature gap-equation:

$$2\Delta(\mathbf{k}') = - \sum_{\mathbf{k}} V(\mathbf{k}', \mathbf{k}; \omega) \frac{\Delta(\mathbf{k})}{\sqrt{[\varepsilon(\mathbf{k}) - \varepsilon_F]^2 + \Delta(\mathbf{k})^2}},$$

the electron-phonon interaction must be large when  $\Delta(\mathbf{k})$  and  $\Delta(\mathbf{k}')$  have the same sign, and small when they have opposite signs. The main pairing interaction is usually believed to be associated with the exchange of spin fluctuations, because it is repulsive and seems to peak for large momentum transfers<sup>10</sup>. In the RPA, its form is

$$V_{sf}(\mathbf{q}, \omega) = \frac{3}{2} \bar{U}^2 \frac{\chi_0(\mathbf{q}, \omega)}{1 - \bar{U} \chi_0(\mathbf{q}, \omega)}$$

where the band susceptibility  $\chi_0(\mathbf{q}, \omega)$  is supposed to be peaked near  $\mathbf{q} = (\frac{\pi}{a}, \frac{\pi}{a})$ . On the basis of models derived from LDA calculations<sup>13-15</sup>, as well as LDA linear-response calculations<sup>16</sup>, we shall argue that this is the case for the so-called buckling mode, which for YBa<sub>2</sub>Cu<sub>3</sub>O<sub>7</sub> and  $\mathbf{q}=\mathbf{0}$  is the 330 cm<sup>-1</sup> ( $\hbar\omega \sim 40$  meV) oxygen out-of-plane and out-of-phase mode. Although the interaction of electrons with this mode is proportional

to the static dimple (YBa<sub>2</sub>Cu<sub>3</sub>O<sub>7</sub>;  $\delta = 7^\circ$ ) or buckle (doped La<sub>2</sub>CuO<sub>4</sub> LTO phase), and hence expected to be small, Raman and neutron-scattering experiments, as well as LDA calculations, have shown it to be relatively strong.

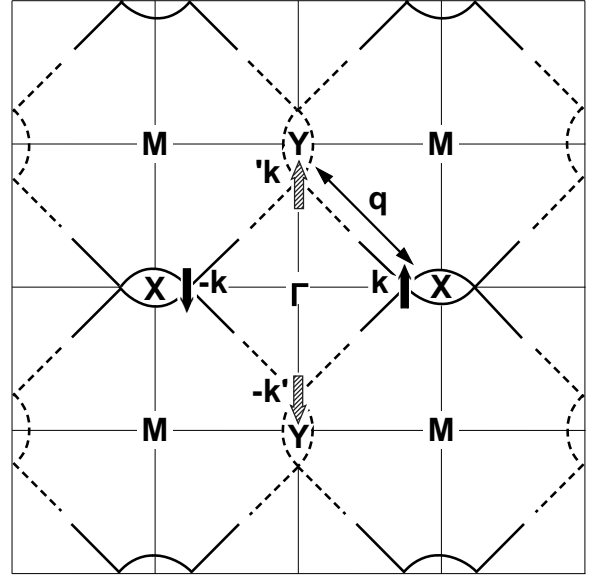


FIG. 1. Fermi surface of an optimally doped CuO<sub>2</sub> superconductor (schematic). The energy bands are nearly flat around X and Y (slightly bifurcated saddle-points). For the experimentally observed *d*<sub>*x*<sup>2</sup>-*y*<sup>2</sup>-wave pairing, the superconducting gap  $\Delta(\mathbf{k})$  has opposite signs on the parts of the Fermi surface which are shown in full- and broken-line. The scattering of a Cooper pair at  $(\mathbf{k}, -\mathbf{k})$  to one at  $(\mathbf{k}', -\mathbf{k}')$  is indicated. The pair-interaction  $V(\mathbf{k}, \mathbf{k}')$  which sustains this gap-anisotropy must be repulsive for momentum transfers  $\mathbf{q} \equiv \mathbf{k}' - \mathbf{k}$  connecting full and broken parts, and attractive for  $\mathbf{q}$ 's connecting full with full, and broken with broken parts. The first property is presumably provided by the Coulomb repulsion and the second, we argue, could be provided by the interaction between near-saddle-point electrons and buckling modes.</sub>

Fig. 2 specifies our generic tight-binding model for the electronic band structure of a single CuO<sub>2</sub>-plane. In the upper part of the 2nd row are shown the four  $\sigma$ -orbitals,  $|y\rangle \equiv O3_y$ ,  $|d\rangle \equiv Cu_{x^2-y^2}$ ,  $|x\rangle \equiv O2_x$ , and  $|s\rangle \equiv Cu_{s-(3z^2-1)}$ , and in the lower part, the  $|d\rangle$  orbital and two of the  $\pi$ -orbitals,  $|z\rangle \equiv O2_z$  and  $|xz\rangle \equiv Cu_{xz}$ , seen from the side of the plane. When merely the *pd* $\sigma$  and *pd* $\pi$  hopping integrals  $t_{xd}=t_{yd} \equiv t_{pd}=1.6$  eV and  $t_{z,xz}=t_{z,yz}=0.7$

eV indicated in the 1st column are taken into account, the band structure and corresponding constant-energy contours, in Fig. 3, shown in the 1st columns arise: The  $\sigma$ -orbitals give rise to a bonding, a non-bonding, and an anti-bonding  $O_x\text{-Cu}_{x^2-y^2}\text{-O}_y$  band plus a high-lying  $\text{Cu}_{s-(3z^2-1)}$  level (full lines), and the  $\pi$ -orbitals give rise to two decoupled pairs of bonding anti-bonding bands which disperse in either the  $k_x$  or  $k_y$  direction (stippled lines). The orbital energies (in eV and with respect to the energy of the  $\text{Cu}_{x^2-y^2}$  orbital) are indicated at the relevant points of the band structure. The conduction

band is the anti-bonding  $pd\sigma$  band and the Fermi level will be close to the saddle-point at X ( $\pi,0$ ). In the 1st column, this saddle-point is well above the top of the  $pd\pi$ -band and is *symmetric*, in the sense that the absolute values of the band masses in the  $k_x$  and  $k_y$  directions are equal. This means that the constant-energy contour through the saddle-point is a square with corners at X and Y. This is shown in 1st row of Fig. 3. In the 2nd columns, the strong hoppings ( $t_{sp}=2.3$  eV) between the high-energy  $\text{Cu}_{s-(3z^2-1)}$  orbital and the  $\text{O}_{2x}$  and  $\text{O}_{3y}$  orbitals and the tiny  $\text{O}_{2z}$  and  $\text{O}_{3z}$  hopping are included.

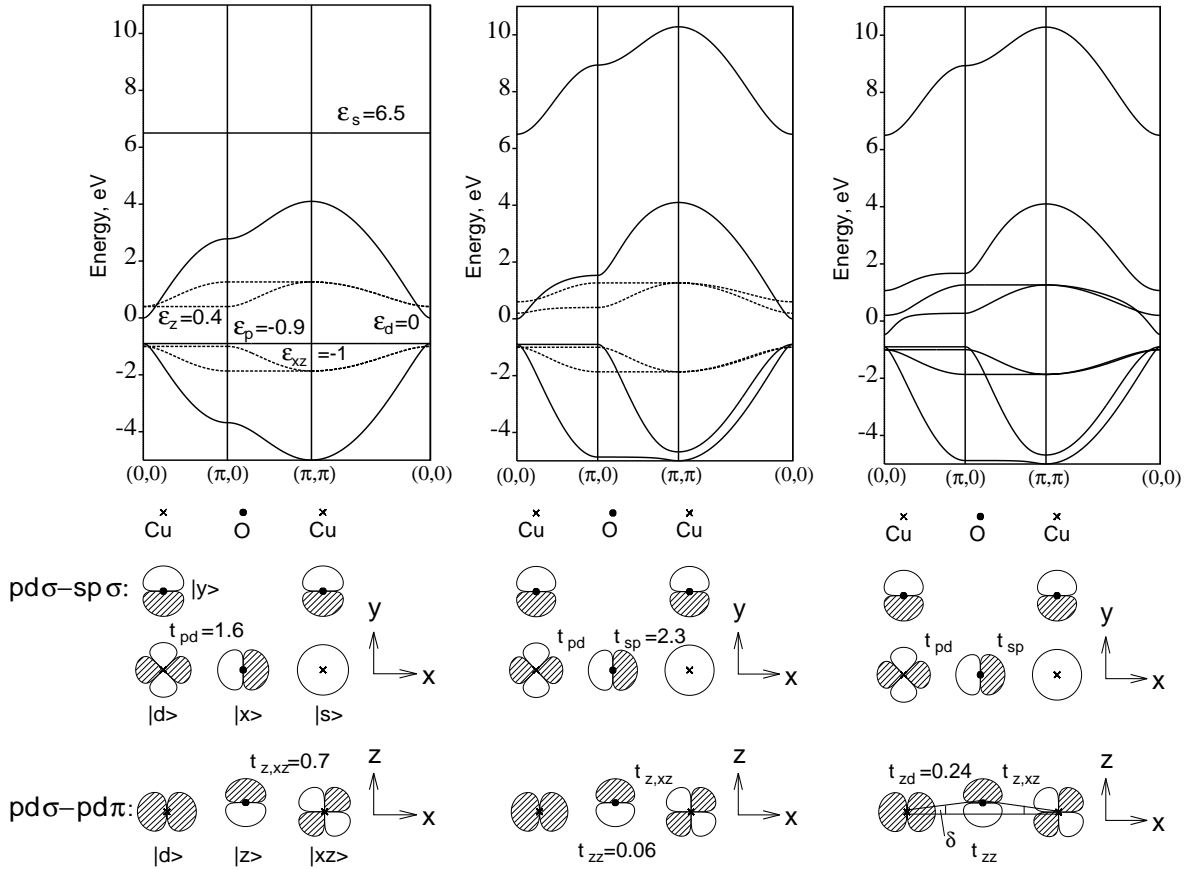


FIG. 2. Eight-band Hamiltonian for a single  $\text{CuO}_2$  plane (2nd row) and synthesis of its band structure (1st row). The 1st column shows uncoupled  $pd\sigma$  ( $O_x\text{-Cu}_{x^2-y^2}\text{-O}_y$ ),  $sp\sigma$  ( $\text{Cu}_s$ ), and  $pd\pi$  ( $\text{Cu}_{xz}\text{-O}_z$  and  $\text{Cu}_{yz}\text{-O}_z$ ) bands. In the 2nd column, the coupling ( $t_{sp}$ ) of the  $\text{Cu}_s$  orbital to the  $pd\sigma$  band is included. In the 3rd column, also the coupling ( $t_{zd}$ ) between  $\sigma$ - and  $\pi$ -bands induced by a static dimple ( $\delta = 7^\circ$ ) is included. Modulation of the latter gives rise to interaction with the buckling mode. All energies are in eV.

This depresses the conduction band near  $(\pi, 0)$  and thereby increases the mass towards  $\Gamma$  ( $0, 0$ ) and decreases it towards M ( $\pi, \pi$ ); the saddle-point becomes *asymmetric* and the constant-energy contours now bulge towards  $\Gamma$ . With the flat part of the conduction band just straddling off the top of a  $\pi$ -band, even a weak dimple or buckle of the plane will introduce considerable hybridization between the  $\sigma$  and  $pd\pi$  bands. This is seen in the

3rd columns where we have turned on the weak  $\text{Cu}_{x^2-y^2}\text{-O}_z$  hoppings ( $t_{zd}=0.24$  eV  $\propto \sin(\delta=7^\circ)$ ). Since the hybridization with the  $\text{Cu}_{xz}\text{-O}_{2z}$   $pd\pi$  band (but not with the lower-lying  $\text{Cu}_{yz}\text{-O}_{3z}$  band) vanishes at X ( $\pi, 0$ ), the saddle-point *bifurcates* away from X and towards  $\Gamma$ , once  $\delta$  exceeds a critical value ( $\sim 4^\circ$  in  $\text{YBa}_2\text{Cu}_3\text{O}_7$ ). The conduction band thereby becomes very flat in a region around X (and Y) extending towards  $\Gamma$ .

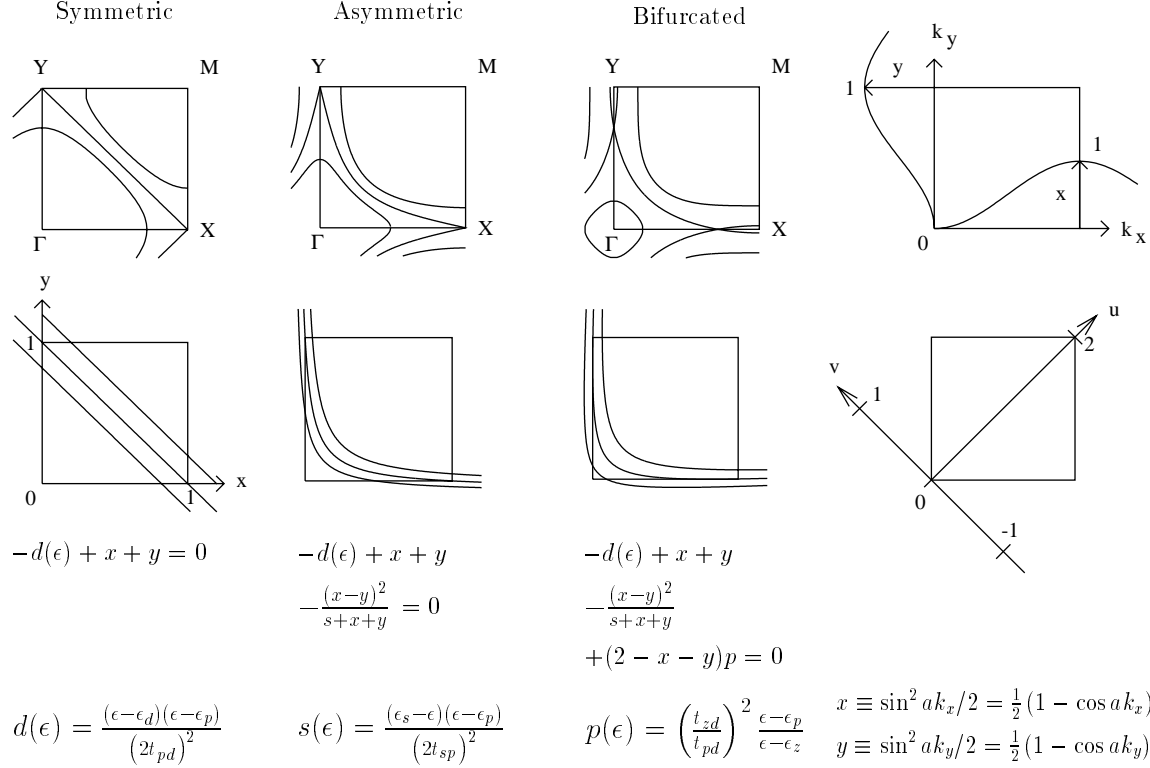


FIG. 3. Constant-energy contours in  $(k_x, k_y)$ -space (1st row), as well as in an  $(x, y)$ -space where the constant-energy contours are hyperbolas (2nd row). The constant-energy contours shown are those of the second band from the top in Fig. 2 and for energies close to that of the saddle-point at X  $(\pi, 0)$ , which is the Fermi level for optimal doping. The coordinate transformation is specified in the 4th column and the analytical expressions for the constant-energy contours are given in the 3rd and 4th rows. The functions  $d(\epsilon)$ ,  $s(\epsilon)$ , and  $p(\epsilon)$  describe respectively the  $pd\sigma$ ,  $sp\sigma$ , and  $\sigma\pi$  scatterings. In the first column  $s=\infty$ , and  $p=0$ . In the second column  $s=0.6$  and  $p=0$ . In the third column,  $s=0.6$  and  $p=0.14$ .

It is this near degeneracy with the top of a  $\pi$ -band of the saddle-point of the conduction-band, which has  $\sigma$ -character, which causes strong coupling to out-of-plane deformations. How near the  $\sigma$ - $\pi$  degeneracy is, is first of all controlled by the energy of the  $\text{Cu}_{s-(3z^2-1)}$  hybrid and, hence, by the distance of apical oxygen from plane copper. Secondly, if the saddle-point of the  $\sigma$ -band is suppressed below the top of the  $\pi$ -band and part of the Fermi-surface becomes  $\pi$ -like, then a static dimple or buckle will adjust itself through reduction of the  $\pi$ -band width ( $\propto t_{z,zz}$ ) so that the  $\pi$ -band becomes essentially filled. This, we have learned from total-energy LDA calculations<sup>16</sup>.

Although our tight-binding model has 8 orbitals per  $\text{CuO}_2$  unit, the constant-energy contours,  $\epsilon_j(k_x, k_y) = \epsilon$ , have simple analytical expressions. These are given in the bottom rows of Fig. 3 and are expressed in terms of functions,  $d(\epsilon)$ ,  $s(\epsilon)$ , and  $p(\epsilon)$ , which describe the  $dp\sigma$ ,  $sp\sigma$ , and  $\sigma\pi$  scatterings. If we neglect the  $\text{Cu}_{xz}$  and  $\text{Cu}_{yz}$  orbitals the constant-energy contours are merely hyperbolas in a  $(x, y)$ -space defined by:  $x \equiv \frac{1}{2}(1 - \cos ak_x)$  and  $y \equiv \frac{1}{2}(1 - \cos ak_y)$ , and they are shown in the 2nd row of Fig. 3. The bottom rows give the explicit expressions. With this model we can now easily calculate

$$\chi_0''(\mathbf{q}, \omega) = 2\pi \int \frac{d^2k}{BZA} [f(\epsilon(\mathbf{k})) - f(\epsilon(\mathbf{k} + \mathbf{q}))] \times \delta(\epsilon(\mathbf{k} + \mathbf{q}) - \epsilon(\mathbf{k}) - \hbar\omega)$$

as a function of the band shape and the doping. For  $\mathbf{q} \sim \mathbf{Q} \equiv (\pi, \pi)$ , where the Coulomb repulsion is supposed to provide the pairing interaction,  $\chi_0''$  vanishes when  $\epsilon_F$  is below the saddle-point and  $\hbar\omega$  is less than  $\sim \epsilon_{\text{saddle}} - \epsilon_F$  (overdoping). If  $\epsilon_F$  is at or above a saddle-point and this is slightly bifurcated, then  $\chi_0''(\mathbf{q}, \omega)$  has a large, broad peak around  $\mathbf{Q}$  for  $\hbar\omega$  larger than  $\sim \epsilon_F - \epsilon_{\text{saddle}}$ . This peak is due to "nesting" of the flat band near X with the one near Y. This, we believe, gives rise to spin-fluctuations which provide the repulsive, large- $\mathbf{q}$  part of the pairing interaction. For smaller  $\mathbf{q}$  and near-optimal doping,  $\chi_0''(\mathbf{q}, \omega)$  with  $\hbar\omega \sim 40$  meV has high ridges which are caused by the "sliding" of a saddle-point along the Fermi surface. We shall now show that the buckling phonon takes advantage of this part of  $\chi_0''$  and does not feel the peak at large  $\mathbf{q}$  because here, its interaction  $|g(\mathbf{k}, \mathbf{k}')|^2$  vanishes.

The last point is illustrated in Fig. 4 where we have assumed a static dimple like in  $\text{YBa}_2\text{Cu}_3\text{O}_7$ . The left- and right-hand sides show the electronic wave-functions

at X and Y, respectively. The  $\text{Cu}_{s-(3z^2-1)}$  character, irrelevant for our qualitative argument, is neglected, but the weak  $\text{Cu}_{yz}\text{-O}3_z$  and  $\text{Cu}_{xz}\text{-O}2_z$  characters at respectively X and Y are included. As mentioned above, and as can be seen from the figure, there can be no  $\text{Cu}_{xz}\text{-O}2_z$  character at X and no  $\text{Cu}_{yz}\text{-O}3_z$  character at Y. On the right-hand side, we have perturbed the wavefunction at Y by the buckling mode with  $\mathbf{q} = \mathbf{Q}$ . This wave in the  $[1, 1]$ -direction increases/decreases the dimple of every other oxygen row and accordingly modulates the coupling  $t_{zd}$  between each  $\text{O}2_z$  and its neighboring  $\text{Cu}_{x^2-y^2}$  orbitals. The electron-phonon matrix element  $\langle \Psi(X) | \delta(\mathbf{Q}) | \Psi(Y) \rangle$  is seen to have contributions from hopping between orbitals, drawn with thick lines, only and it vanishes because  $\delta(\mathbf{Q}) | \Psi(Y) \rangle$  is even and  $\langle \Psi(X) |$  is odd with respect to a  $y$ -axis through the  $\text{O}2$ 's.

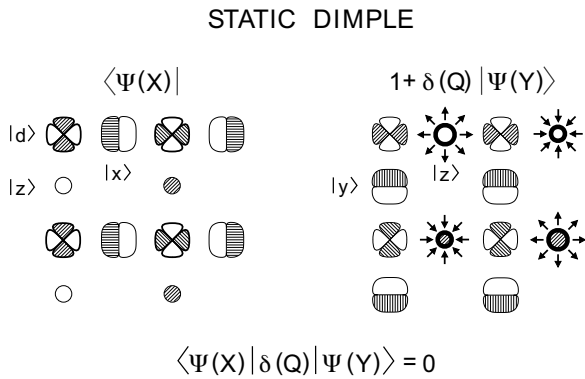


FIG. 4. Schematic illustration of why there is no electron-phonon interaction for the buckling mode with  $\mathbf{Q} \equiv (\pi, \pi)$ .

The strength of the electron-phonon interaction is

$$\lambda = [\pi N(\epsilon_F)]^{-1} \int_{BZ} \frac{d^2 q}{BZA} \gamma(\mathbf{q}, \omega) / \omega(\mathbf{q})^2$$

where

$$N(\epsilon_F) = \int_{FS} \frac{dk}{BZA} |v(\mathbf{k})|^{-1}$$

is the electronic density of states and

$$\begin{aligned} \gamma(\mathbf{q}, \omega) = & 2\pi \int \frac{d^2 k}{BZA} \{f[\epsilon(\mathbf{k})] - f[\epsilon(\mathbf{k} + \mathbf{q})]\} \\ & \times \delta[\epsilon(\mathbf{k} + \mathbf{q}) - \epsilon(\mathbf{k}) - \hbar\omega(\mathbf{q})] |g(\mathbf{k}, \mathbf{k} + \mathbf{q})|^2 \end{aligned}$$

the phonon linewidth. For the  $d$ -wave channel with gap-anisotropy  $\frac{1}{2}(\cos ak_y - \cos ak_x) = x - y$ , a factor  $(x - y)^2$  must be included in the integrand for  $N(\epsilon_F)$ , thus yielding  $N_d(\epsilon_F)$ , and a factor  $(x - y)(x' - y')$  must be included in the integrand for  $\gamma(\mathbf{q}, \omega)$ . Hence for  $g$  constant,  $\lambda_d$  would vanish. For the buckling mode our tight-binding model yields:

$$\begin{aligned} g(\mathbf{k}, \mathbf{k}') = & 2t_{zd} \frac{\epsilon_F - \epsilon_p}{(\epsilon_F - \epsilon_z)(\epsilon_F - \frac{\epsilon_p + \epsilon_d}{2})} \frac{\partial t_{zd} / \partial z_O}{\sqrt{M\omega}} \\ & \times \left[ \sqrt{(1-x)(1-x')} - \sqrt{(1-y)(1-y')} \right], \end{aligned}$$

where for simplicity we have neglected the dispersion of the  $\pi$  bands. It is easy to see that this form vanishes for  $\mathbf{q} = \mathbf{Q}$ , for instance. To further illustrate this form we

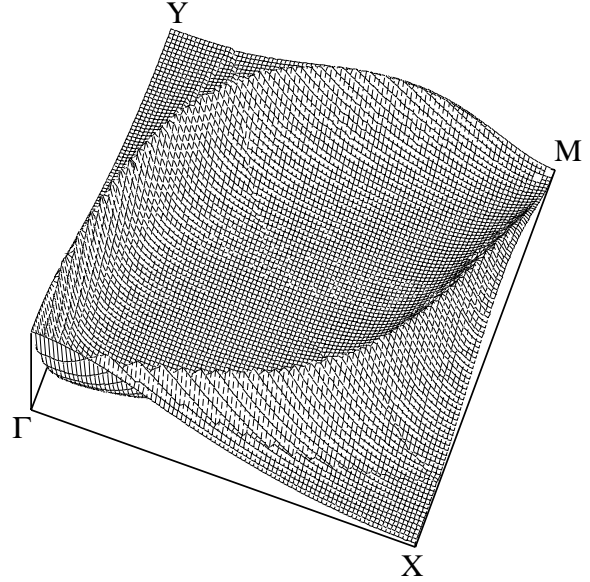


FIG. 5.  $(\mathbf{k} - \mathbf{k}')$ -dependence of the electron-phonon interaction for the out-of phase buckling mode from the six-orbital model.  $\mathbf{k}$  and  $\mathbf{k}'$  were chosen on the  $\text{YBa}_2\text{Cu}_3\text{O}_7$ -type Fermi surface, which lies between the two low hole doping constant-energy contours in the third column of Figure 3.

show in Fig. 5  $g(\mathbf{q}) \equiv \gamma(\mathbf{q}, 0) / \chi_0''(\mathbf{q}, 0)$ , calculated for a band shape with a marginally bifurcated (extended) saddle-point slightly below  $\epsilon_F$ . This  $g$  is seen to have the kind of dispersion required in order to support  $d$ -wave pairing.  $g(\mathbf{k}, \mathbf{k}')$  as given above, factorizes and the double-integral for  $\lambda_d$  may be expressed analytically and the result for  $\omega \rightarrow 0$  is simply:  $\lambda_d = c^2 \omega^{-1} N_d(\epsilon_F)$ , where  $c$  is the factor in front of the square parenthesis in the expression for  $g(\mathbf{k}, \mathbf{k}')$ . This result is *positive definite* for all dopings. For  $\epsilon_F$  approaching a saddle-point at X,  $N_d \rightarrow N$ , so that the strength of the electron-phonon interaction in this  $d$ -channel is as large as in the  $s$ -channel.

Finally, in Fig. 6 we show the phonon spectrum calculated *ab initio* with the linear-response LDA-LMTO method for the idealized infinite-layer compound  $\text{CaCuO}_2$  doped with 0.24 holes per formula unit<sup>16</sup>. In the calculations, this compound developed a static buckle ( $\text{O}2$  up and  $\text{O}3$  down by  $\delta=6^\circ$ ). The uppermost of the three phonon branches marked with spheres is the buckling mode and the numbers written on the modes are the mode  $\lambda_d$ 's. We see that the buckling mode dominates  $\lambda_d$  and that it is large close to  $\Gamma$  along  $\Gamma X$  and vanishes at  $M(\pi, \pi)$ . Numerically we found  $\lambda_d = 0.3$  and  $\lambda_s = 0.4$ .

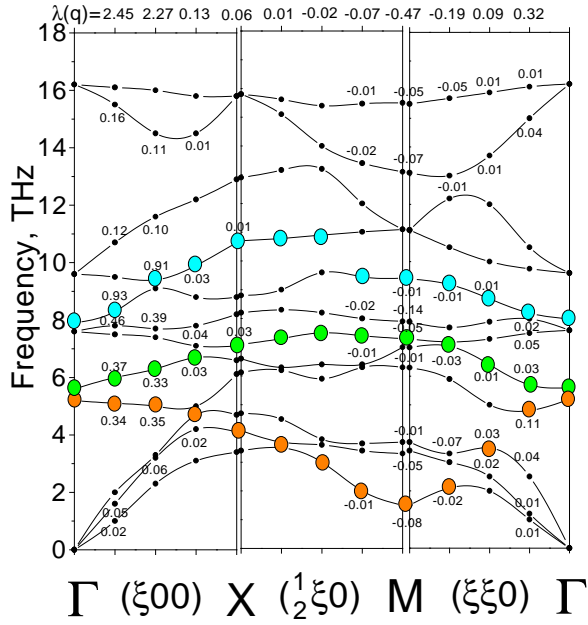


FIG. 6. Phonon modes and the mode  $\lambda_d$  calculated *ab initio* with the linear-response LDA-LMTO method for  $\text{CaCuO}_2$  doped with 0.24 holes.

We conclude that the linear electron-phonon interaction for buckled or dimpled  $\text{CuO}_2$ -planes may support, but is hardly sufficient to cause, high-temperature superconductivity based on  $d_{x^2-y^2}$ -pairing. The most important mode seems to be the buckling mode, because it modulates the saddle-points of the energy bands where the density of states is high and where the superconducting gap is observed to be maximum. The electron-phonon interaction, for this mode, is small or vanishes for momentum transfers  $\mathbf{q}$  near  $(\pi, \pi)$ , and does therefore not interfere with the  $d$ -wave symmetry of the order parameter induced by spin-fluctuation exchange.

- <sup>1</sup> For a recent review, see, *e.g.*, N. M. Plakida, *High-Temperature Superconductivity* (Springer-Verlag, Berlin, 1995).
- <sup>2</sup> C. Thomsen and M. Cardona, in *Physical Properties of High-Temperature Superconductors I*, ed. by D. M. Ginsberg (World Scientific, Singapore, 1989), p. 409.
- <sup>3</sup> C. Frank, in *Physical Properties of High-Temperature Superconductors IV*, ed. by D. M. Ginsberg (World Scientific, Singapore, 1993), p. 189.
- <sup>4</sup> S. I. Vedenev, P. Samuely, S. V. Meshkov, G. M. Eliashberg, A. G. M. Jansen, P. Wyder, *Physica C* **198**, 47 (1992); N. Miyakawa, Y. Shiina, T. Kaneko, N. Tsuda, *J. Phys. Soc. Jpn.* **62**, 2445 (1993).
- <sup>5</sup> C.O. Rodriguez, A.I. Liechtenstein, I.I. Mazin, O. Jepsen, and O.K. Andersen, *Phys. Rev. B* **49**, 4145 (1994).
- <sup>6</sup> R. E. Cohen, W. E. Pickett, H. Krakauer, *Phys. Rev. Lett.* **64**, 2575 (1990).
- <sup>7</sup> O.K. Andersen, A.I. Liechtenstein, C.O. Rodriguez, I.I. Mazin, O. Jepsen, V.P. Antropov, O. Gunnarsson, S. Gopalan, *Physica C* **185-189**, 147 (1991).
- <sup>8</sup> I.I. Mazin, O.K. Andersen, A.I. Liechtenstein, O. Jepsen, V.P. Antropov, S.N. Rashkeev, V.I. Anisimov, J. Zaanen, C.O. Rodriguez, and M. Methfessel; in *Lattice Effects in High- $T_C$  Superconductors*. p. 235 Edts. Y. Bar-Yam, T. Egami, J. Mustre-de Leon, and A.R. Bishop (World Scientific, Singapore, 1993).
- <sup>9</sup> B.G. Levi, *Physics Today* **46**, 17 (1993), and references therein.
- <sup>10</sup> D.J. Scalapino, *Phys. Rep.* **250**, 329 (1995).
- <sup>11</sup> D.J. Scalapino, *J. Phys. Chem. Solids* **56**, 1669 (1995).
- <sup>12</sup> N. Bulut and D.J. Scalapino, *Phys. Rev. B* **54**, 14971 (1996).
- <sup>13</sup> O.K. Andersen, O. Jepsen, A.I. Liechtenstein, and I.I. Mazin, *Phys. Rev. B* **49**, 4145 (1994).
- <sup>14</sup> O.K. Andersen, A.I. Liechtenstein, O. Jepsen, and F. Poulsen, *J. Phys. Chem. Solids* **56**, 1573 (1995).
- <sup>15</sup> O.K. Andersen, S.Y. Savrasov, O. Jepsen, and A.I. Liechtenstein, *J. Low Temp. Phys.* **105**, 285 (1996).
- <sup>16</sup> S.Y. Savrasov and O.K. Andersen, *Phys. Rev. Lett.* **77**, 4420 (1996).